Mathematical models of retinitis pigmentosa: the trophic factor hypothesis

Paul Roberts

Publication date
10-06-2023

Document Version
Accepted version

Citation for this work (American Psychological Association 7th edition)
Roberts, P. (2021). *Mathematical models of retinitis pigmentosa: the trophic factor hypothesis* (Version 1). University of Sussex. https://hdl.handle.net/10779/uos.23484899.v1

Published in
Journal of Theoretical Biology

Link to external publisher version
https://doi.org/10.1016/j.jtbi.2021.110938

Mathematical Models of Retinitis Pigmentosa: The Trophic Factor Hypothesis
Journal of Theoretical Biology
Supplementary Material

Paul A. Roberts*[1]

[1]School of Life Sciences, University of Sussex, John Maynard Smith Building, Brighton, BN1 9QG, UK

S1 Justification of parameter values

- **Retinal radial position, R:** chosen to be 1.2×10^{-2} m, the average radius of the human eye (Oyster, 1999).
- **Eccentricity of the ora serrata, Θ:** chosen to be 1.33 rad, the extent of the retina along the horizontal meridian in the temporal direction, as measured by Curcio et al. (1990).
- **Trophic factor diffusivity, D_f:** the protein RdCVF has been found to come in four forms, two short forms, RdCVF-S and RdCVF2-S (produced by rods, but not by cones), and two long forms, RdCVF-L and RdCVF2-L (produced by rods and cones; Chalmel et al., 2007; Léveillard et al., 2004). It is the short forms that enhance cone glucose uptake and for which cones rely upon rods for a supply, and the first of these, RdCVF-S, which is the more effective of the two, RdCVF2-S acting in an additive (as opposed to a synergistic) fashion (Chalmel et al., 2007; Léveillard et al., 2004). Therefore, we include only the RdCVF-S form in our models. To the best of our knowledge, no measurements have been published for the diffusivity of RdCVF in any of its forms; however, the molecular weight of RdCVF-S has been measured to be 17 kDa (Léveillard et al., 2004). The protein myoglobin also has a molecular weight of 17 kDa (Zaia et al., 1992), and its diffusivity has been measured; therefore, we assume that the diffusivity of RdCVF-S is the same as that of myoglobin. Jürgens et al. (1994) have measured myoglobin diffusivity to be 1.17×10^{-11} m^{2}s^{-1} at 22°C in diaphragm muscle. Using the Q_{10} rule[1] with $Q_{10} = 1.3$, gives a value of 1.73×10^{-11} m^{2}s^{-1} at 37°C (body temperature, Jürgens et al., 1994), which is the value we choose for D_f (see also, McGuire and Secomb, 2001).
- **Rate of trophic factor decay, η:** to the best of our knowledge, this parameter has not been measured; however, Eden et al. (2011) have measured the half-life dynamics for a range of proteins in living human cells. In their experiments, cells were treated with the drug cisplatin, which reduces cell growth by 85%, such that the measured reduction in protein concentration is mainly due to degradation, rather than cell growth-induced dilution. Protein half-lives in the range 0.9–20.5 hr were measured, corresponding to exponential decay rates in the range 9.39×10^{-6}–2.14×10^{-4} s^{-1}. Similarly, Dörrbaum et al. (2018) measured protein half-lives in rat primary hippocampal, neuron-enriched and glia-enriched cultures ranging from 17 hr–110 days, the majority lying in the range 1–20 days, corresponding to exponential decay rates in the range 4.01×10^{-7}–8.02×10^{-6} s^{-1}. These values are smaller than (though of a similar order of magnitude to) those measured by Eden et al.

*Corresponding author
E-mail address: p.a.roberts@univ.oxon.org (Paul A. Roberts)

[1] $Q_{10} = (\frac{D_2}{D_1})^{(\frac{10}{T_2 - T_1})}$, where D_1 (D_2) is the diffusivity at temperature T_1 (T_2).

(2011). We assume the values measured by Eden et al. (2011) to be more typical of the human retina since they were measured in human cells, taking the rate of trophic factor decay to be 5.13×10^{-5} s^{-1} (the mean of the rates corresponding to the half-lives measured by Eden et al., 2011).

- **Rate of trophic factor consumption by cones, β:** to the best of our knowledge, this parameter has not been measured. We choose the rate of trophic factor consumption such that its dimensionless value is four orders of magnitude greater than the rate of trophic factor decay, η, ensuring that the trophic factor consumption term dominates over the decay term, as would be expected biologically. Thus, we choose the dimensionless value $\beta^* = 1.79 \times 10^6$, which corresponds to a dimensional value of $\beta = 4.62 \times 10^{-12}$ m^{2}photoreceptors^{-1}s^{-1}.

- **Rate of trophic factor production by rods, α:** to the best of our knowledge, this parameter has not been measured. In the absence of further information, we choose α such that the trophic factor production term is of the same order of magnitude as (and hence balances with) the consumption term, as would be expected biologically. This leaves a degree of freedom, and we choose α such that the mean trophic factor concentration $\tilde{f}_A = 1 \times 10^{-4}$ M, for numerical convenience. Thus, we choose $\alpha = 1.81 \times 10^{-17}$ Mm^{2}photoreceptors^{-1}s^{-1}.

- **Rate of trophic factor supply from treatment, ξ:** to the best of our knowledge, this parameter has not been measured. Therefore, we choose values on the order of magnitude of the critical treatment rate, ξ_{crit}, as predicted by numerical and analytical solutions to the steady-state problem (see Section 3.2.2).

- **Rate of mutation-induced rod degeneration, ϕ_r:** the rate of rod degeneration in the healthy human retina has been investigated by Curcio et al. (1993), who measured a 31% reduction in the total number of rods in the central 28.5 degrees of vision between the ages of 34 and 90 yr, corresponding to an exponential decay rate of 2.10×10^{-10} s^{-1}. Since the rate of rod degeneration is accelerated in RP we take this value as a lower bound and assume that the rate of mutation-induced rod degeneration is two orders of magnitude higher, that is $\phi_r = 2.10 \times 10^{-8}$ s^{-1}. This places the timescale of the resultant cone loss on the order of decades (see Fig. 9(a)), in line with *in vivo* progression rates.

- **Growth rate of cone OS (phases 1 and 2), μ_1 and μ_2:** Guérin et al. (1993) measured cone OS regrowth in rhesus monkeys following a 7-day retinal detachment period. In their study, rod and cone OS regrowth occurred simultaneously. In the absence of further information, we assume cone OS regrowth dynamics are the same whether rod OS are present or absent initially. RdCVF treatment only aids cone regeneration since rods remain unhealthy due to their expression of a mutant gene; therefore, we only consider cone regeneration here. As described in Section 2, we found that cone OS regrowth is well-described by a two-phase model. Phase 1, constant growth, occurs for cone OS lengths between 0 and 0.33 as a proportion of their full length, while phase 2, hyperbolic growth, occurs for cone OS lengths between 0.33 and 1 as a proportion of their full length (see Section 2 for more details). Cone OS length was zero immediately following reattachment (at 0 days) and reached 33% of its healthy length after 7 days. Thus, we can directly calculate the phase 1 constant growth rate as $\mu_1 = 1.60 \times 10^{-11}$ ms^{-1}. The phase 2 growth term was fitted to the data using the Matlab routine `fminsearch`, taking the data point at 7 days (33% length) as the initial condition and seeking to minimise the mean squared error between the model and the remaining data points to give $\mu_2 = 3.07 \times 10^{-12}$ ms^{-1} (see Fig. S1). We note that it takes much longer to regrow a cone OS following the re-establishment of RdCVF supply than to completely shed it during RdCVF deprivation since in the latter case shedding occurs in the absence of regeneration while in the former case regeneration is accompanied by shedding for lengths greater than 33%, slowing the recovery of OS length (which reaches 80% of the healthy length by day 150, Guérin et al., 1993).

- **Rate of trophic factor starvation-induced cone OS degeneration, δ_L:** while the rate of cone OS degeneration due specifically to RdCVF starvation has not, to the best of our knowledge, been measured, the rate of cone OS shedding under healthy conditions in humans and a number of animal species has been measured. We assume that, in the absence of sufficient RdCVF, cone OS regeneration ceases, while cone OS shedding continues at its healthy rate. Kocaoglu et al. (2016) studied cone OS shedding in the living human eye. They found that it takes between 12.67 and 16.7 days to shed (and hence renew) an entire cone OS. Based on the values given in Kocaoglu et al. (2016), we assume an average time of 14.5 days (1.25×10^6 s) to shed a full cone OS, corresponding to a rate of $\delta_L = 2.34 \times 10^{-11}$ ms^{-1}. These measurements agree well with the rates of cone OS

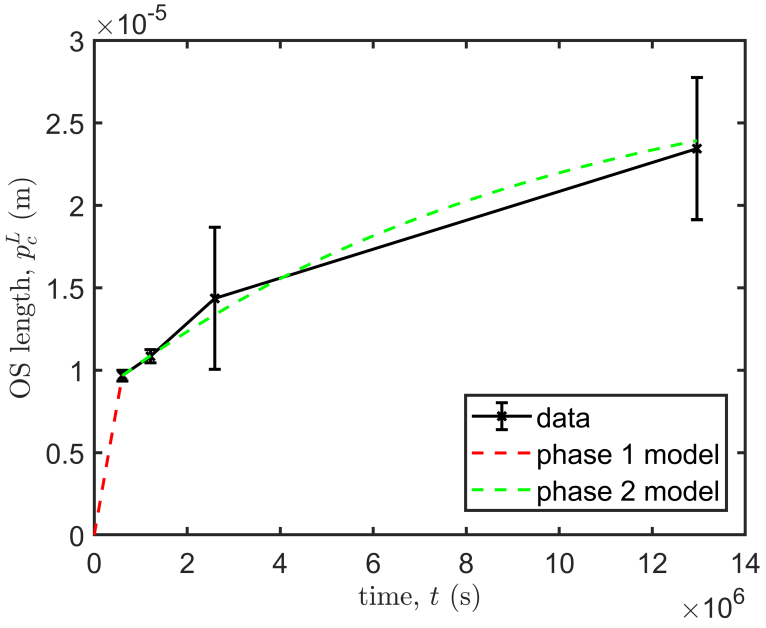

Figure S1: Graph to show model fit to cone OS regrowth data from Guérin et al. (1993). Mean data are plotted as crosses, while the error bars demarcate the standard deviation. Phase 1 — constant growth: $\dot{p}_c^L = \mu_1$; and phase 2 — hyperbolic growth: $\dot{p}_c^L = \mu_2(1 - p_c^L/\tilde{p}_c^L)$, where dot($\dot{}$) denotes the temporal partial derivative. Parameter values: $\mu_1 = 1.60 \times 10^{-11}$ ms^{-1}, $\mu_2 = 3.07 \times 10^{-12}$ ms^{-1} and $\tilde{p}_c^L = 2.93 \times 10^{-5}$ m.

regeneration measured by Jonnal et al. (2010, 2012) and Pircher et al. (2011) in living humans, which balances shedding to maintain a roughly constant OS length.

- **Rate of trophic factor starvation-induced cone degeneration, δ:** the rate of cone degeneration due specifically to RdCVF starvation has not, to the best of our knowledge, been measured; however, given that cone OS would be lost in about 14.5 days (see discussion above, Kocaoglu et al., 2016) and given that cones may be assumed to be mostly healthy immediately following OS loss, taking further time for the rest of the cell to degenerate, a half-life of 28 days seems reasonable. This results in a cone degeneration rate of 2.87×10^{-7} s^{-1} (noting that half-lives from 10–100 days all result in rates of degeneration of $\sim O(10^{-7})$ s^{-1}).

- **Healthy cone OS length, $\tilde{p}_c^L$:** Kocaoglu et al. (2016) measured cone OS lengths in the eyes of three healthy human subjects, the average lengths being $25.5 \pm 1.7 \times 10^{-6}$ m, $30.9 \pm 1.8 \times 10^{-6}$ m and $31.6 \pm 1.5 \times 10^{-6}$ m. We take the healthy cone OS length to be the mean of these values, $\tilde{p}_c^L = 29.3 \times 10^{-6}$ m. We note that while we have chosen a biologically realistic value for this parameter for the dimensional model, the value chosen makes no difference to the parameter values in the non-dimensional model due to the way in which the parameter is cancelled out through non-dimensionalisation.

- **Trophic factor threshold concentration, f_{crit}:** the minimal RdCVF concentration required to maintain cones in health has not, to the best of our knowledge, been measured. In the absence of further information, we choose two possible values for f_{crit}. The first value ($f_{\text{crit}} = 3 \times 10^{-9}$ M) is taken to lie just below the minimum RdCVF concentration at steady-state under healthy conditions and in the absence of treatment (i.e. where $p_r = \tilde{p}_r(\theta)$, $p_c = \tilde{p}_c(\theta)$ and $\xi = 0$), which occurs at the centre of the fovea ($\theta = 0$ rad). The second value ($f_{\text{crit}} = 3 \times 10^{-5}$ M) is taken to be 10^4 times larger than the first value, lying just below the minimum trophic factor concentration away from the fovea ($\theta > 0.13 \times \Theta$ rad). See Section 3.2 for more details.

- **Rod and cone profile parameters, B_1, B_2, B_3, b_1, b_2, b_3:** determined by fitting the functions $p_r = \tilde{p}_r(\theta)$ and

$p_c = \tilde{p}_c(\theta)$ to Curcio et al. (1990)'s measurements of the mean rod and cone distributions along the temporal horizontal meridian in healthy humans using the Trust-Region Reflective algorithm in Matlab's curve fitting toolbox.

- **Mean trophic factor concentration, $\tilde{f}_A$:** calculated as the mean RdCVF concentration in the dimensional model at steady-state under healthy conditions and in the absence of treatment (i.e. where $p_r = \tilde{p}_r(\theta)$, $p_c = \tilde{p}_c(\theta)$ and $\xi = 0$).
- **Mean photoreceptor density, $\tilde{p}_A$:** calculated as the mean photoreceptor density across the retina under healthy conditions, that is, the mean of $\tilde{p}_r(\theta) + \tilde{p}_c(\theta)$.
- **Degenerate patch boundaries (rods and cones), θ_{r_1}, θ_{r_2}, θ_{c_1} and θ_{c_2}:** chosen to explore disease progression following the loss of patches of rods and/or cones. Selected such that $0 \leq \theta_{r_1} < \theta_{r_2} \leq \Theta$ (rad) and $0 \leq \theta_{c_1} < \theta_{c_2} \leq \Theta$ (rad).
- **Position of left- and right-hand limits of local treatment, θ_{treat_1} and θ_{treat_2}:** chosen to explore the effects of local trophic factor treatment upon cone degeneration and cone OS recovery. Selected such that $0 \leq \theta_{\text{treat}_1} < \theta_{\text{treat}_2} \leq \Theta$ (rad).
- **Time at which treatment first applied, t_{crit}:** chosen to explore the effect of trophic factor treatment at a given stage of retinal degeneration. Selected such that $t_{\text{crit}} > 0$ s.

S2 Asymptotic analyses (continued)

Here we consider St-st Cases 2-8 from Section 3.1. In each case the same approach is taken as in Appendix A. Where the analysis differs from that in Appendix A we explain the difference, otherwise the results are simply stated.

In the sections that follow (S2.1–S2.7) we will use the following parameters (in addition to those defined in Appendix A), defined here for ease of reference:

- $K := e^{\varepsilon^{-1}\sqrt{c_1}(\theta_{r_2}-\theta_{r_1})}$;
- $B := 1 + \varepsilon^{\frac{1}{2}}\sqrt{\frac{\eta}{D_f c_1}}$;
- $\bar{B} := 1 + \varepsilon^{\frac{1}{2}}\sqrt{\frac{\eta}{D_f \bar{c}_1}}$;
- $Q := \varepsilon^{\frac{1}{2}}\sqrt{\frac{\eta}{D_f c_1}} - 1 = B - 2$;
- $\bar{Q} := \varepsilon^{\frac{1}{2}}\sqrt{\frac{\eta}{D_f \bar{c}_1}} - 1 = \bar{B} - 2$;
- $M := e^{\varepsilon^{-1/2}\sqrt{\frac{\eta}{D_f}}(\theta_{r_2}-\theta_{r_1})}$.

S2.1 St-st Case 2: narrow patch of rod loss without treatment

In this case there is no centre-outer region, and the left-centre-inner and right-centre-inner regions coalesce into a single centre-inner region (see Fig. A.1(b)).

Left- and Right-Outer:

$$f_0(\theta) = \frac{\alpha B_3 \theta e^{-b_3\theta}}{\beta B_2 e^{-b_2\theta}}, \tag{S1}$$

Left-Inner:

$$f_0(\theta) = A_1 e^{\varepsilon^{-1}\sqrt{c_1}(\theta-\theta_{r_1})} + \frac{c_2}{c_1}, \tag{S2}$$

Centre-Inner:

$$f_0(\theta) = A_3 e^{-\varepsilon^{-1}\sqrt{c_1}(\theta-\theta_{r_1})} + A_4 e^{\varepsilon^{-1}\sqrt{c_1}(\theta-\theta_{r_2})}, \tag{S3}$$

Right-Inner:

$$f_0(\theta) = A_8 e^{-\varepsilon^{-1}\sqrt{\bar{c}_1}(\theta-\theta_{r_2})} + \frac{\bar{c}_2}{\bar{c}_1}, \tag{S4}$$

where:

$$\begin{aligned}
A_1 &= \left(1+\sqrt{\frac{c_1}{\bar{c}_1}}\right)^{-1}\left[\frac{c_2}{2c_1}K^{-2}\left(\sqrt{\frac{c_1}{\bar{c}_1}}-1\right)+\frac{\bar{c}_2}{\bar{c}_1}K^{-1}\right]-\frac{c_2}{2c_1},\\
A_3 &= \frac{c_2}{2c_1},\\
A_4 &= \left(1+\sqrt{\frac{c_1}{\bar{c}_1}}\right)^{-1}\left[\frac{c_2}{2c_1}K^{-1}\left(\sqrt{\frac{c_1}{\bar{c}_1}}-1\right)+\frac{\bar{c}_2}{\bar{c}_1}\right],\\
A_8 &= -\left(1+\sqrt{\frac{c_1}{\bar{c}_1}}\right)^{-1}\left[\frac{c_2}{2c_1}K^{-1}\left(\sqrt{\frac{c_1}{\bar{c}_1}}-1\right)+\frac{\bar{c}_2}{\bar{c}_1}\right]\sqrt{\frac{c_1}{\bar{c}_1}}+\frac{c_2}{2c_1}\sqrt{\frac{c_1}{\bar{c}_1}}K^{-1},
\end{aligned}$$

Left-Composite:

$$f_{0_{left-comp}}(\theta) = \frac{\alpha B_3 \theta e^{-b_3\theta}}{\beta B_2 e^{-b_2\theta}} + A_1 e^{\varepsilon^{-1}\sqrt{c_1}(\theta-\theta_{r_1})}, \tag{S5}$$

Centre-Composite is identical with the centre-inner,
Right-Composite:

$$f_{0_{right-comp}}(\theta) = \frac{\alpha B_3 \theta e^{-b_3\theta}}{\beta B_2 e^{-b_2\theta}} + A_8 e^{-\varepsilon^{-1}\sqrt{\bar{c}_1}(\theta-\theta_{r_2})}, \tag{S6}$$

Minimal Cone Degenerate Patch Left Boundary:

$$\theta_{\text{crit}_1} = \theta_{r_1} + \frac{\varepsilon}{\sqrt{c_1}}\log\left(A_1^{-1}\left(f_{\text{crit}} - \frac{c_2}{c_1}\right)\right), \text{ for } f_{\text{crit}} \geq A_1 + \frac{c_2}{c_1}, \tag{S7}$$

$$f_{\text{crit}} = A_3 e^{-\varepsilon^{-1}\sqrt{c_1}(\theta_{\text{crit}_1}-\theta_{r_1})} + A_4 e^{\varepsilon^{-1}\sqrt{c_1}(\theta_{\text{crit}_1}-\theta_{r_2})}, \text{ for } f_{\text{crit}} \leq A_1 + \frac{c_2}{c_1}, \tag{S8}$$

Maximal Cone Degenerate Patch Right Boundary:

$$f_{\text{crit}} = A_3 e^{-\varepsilon^{-1}\sqrt{c_1}(\theta_{\text{crit}_2}-\theta_{r_1})} + A_4 e^{\varepsilon^{-1}\sqrt{c_1}(\theta_{\text{crit}_2}-\theta_{r_2})}, \text{ for } f_{\text{crit}} \leq A_8 + \frac{\bar{c}_2}{\bar{c}_1}, \tag{S9}$$

$$\theta_{\text{crit}_2} = \theta_{r_2} - \frac{\varepsilon}{\sqrt{\bar{c}_1}}\log\left(A_8^{-1}\left(f_{\text{crit}} - \frac{\bar{c}_2}{\bar{c}_1}\right)\right), \text{ for } f_{\text{crit}} \geq A_8 + \frac{\bar{c}_2}{\bar{c}_1}, \tag{S10}$$

where Eqs. (S8) and (S9) must be solved implicitly for θ_{crit_1} and θ_{crit_2} respectively,

- when $f_{\text{crit}} \geq A_1 + \frac{c_2}{c_1}$, $\theta_{\text{crit}_1} \leq \theta_{r_1}$;
- when $f_{\text{crit}} < A_1 + \frac{c_2}{c_1}$, $\theta_{\text{crit}_1} > \theta_{r_1}$;
- when $f_{\text{crit}} \geq A_8 + \frac{\bar{c}_2}{\bar{c}_1}$, $\theta_{\text{crit}_2} \geq \theta_{r_2}$;
- when $f_{\text{crit}} < A_8 + \frac{\bar{c}_2}{\bar{c}_1}$, $\theta_{\text{crit}_2} < \theta_{r_2}$.

S2.2 St-st Case 3: wide patch of rod and cone loss without treatment

In this case, $G(\theta) = H(\theta_{c_1} - \theta) + H(\theta - \theta_{c_2})$ (and $F(\theta) = H(\theta_{r_1} - \theta) + H(\theta - \theta_{r_2})$ as before), where $\theta_{c_1} = \theta_{r_1}$ and $\theta_{c_2} = \theta_{r_2}$. The asymptotics for the rod and cone loss case, both here and in S2.3, is valid in the region $\theta \in (\sim 0.16, 1-\varepsilon)$.

We decompose into the same regions as in Appendix A (see Fig. A.1(c)); however, the left- and right-centre-inner regions are $O(\varepsilon^{1/2})$ width in this case. This is because, in the absence of cones in the central region, we must seek a dominant balance between the diffusion and decay terms. Thus, the new scaling on θ in the left-centre-inner region is: $\hat{\theta}' = \varepsilon^{-1/2}(\theta - \theta_{r_1})$; while the new scaling on θ in right-centre-inner region is: $\bar{\theta}' = \varepsilon^{-1/2}(\theta - \theta_{r_2})$; while the regular perturbation expansion for f in the central region is

$$f(\theta) = f_0(\theta) + \varepsilon^{1/2} f_1(\theta) + O(\varepsilon). \tag{S11}$$

Perturbation expansions are not required for rods and cones in this region since they are absent here. The scalings on θ and the regular perturbation expansions in the left-inner and right-inner regions are the same as in Appendix A.

Left- and Right-Outer:

$$f_0(\theta) = \frac{\alpha B_3 \theta e^{-b_3\theta}}{\beta B_2 e^{-b_2\theta}}, \tag{S12}$$

Left-Inner:

$$f_0(\theta) = \frac{c_2}{c_1}\left(1 + \left[\left(1 + \varepsilon^{1/2}\sqrt{\frac{\eta}{D_f c_1}}\right)^{-1} - 1\right] e^{\varepsilon^{-1}\sqrt{c_1}(\theta - \theta_{r_1})}\right), \tag{S13}$$

Left-Centre-Inner:

$$f_0(\theta) = \frac{c_2}{c_1}\left(1 + \varepsilon^{1/2}\sqrt{\frac{\eta}{D_f c_1}}\right)^{-1} e^{-\varepsilon^{-1/2}\sqrt{\frac{\eta}{D_f}}(\theta - \theta_{r_1})}, \tag{S14}$$

Centre-Outer:

$$f_0(\theta) = 0, \tag{S15}$$

Right-Centre-Inner:

$$f_0(\theta) = \frac{\bar{c}_2}{\bar{c}_1}\left(1 + \varepsilon^{1/2}\sqrt{\frac{\eta}{D_f \bar{c}_1}}\right)^{-1} e^{\varepsilon^{-1/2}\sqrt{\frac{\eta}{D_f}}(\theta - \theta_{r_2})}, \tag{S16}$$

Right-Inner:

$$f_0(\theta) = \frac{\bar{c}_2}{\bar{c}_1}\left(1 + \left[\left(1 + \varepsilon^{1/2}\sqrt{\frac{\eta}{D_f \bar{c}_1}}\right)^{-1} - 1\right] e^{-\varepsilon^{-1}\sqrt{\bar{c}_1}(\theta - \theta_{r_2})}\right), \tag{S17}$$

Left-Composite:

$$f_{0_{left-comp}}(\theta) = \frac{\alpha B_3 \theta e^{-b_3\theta}}{\beta B_2 e^{-b_2\theta}} + \frac{c_2}{c_1}\left[\left(1 + \varepsilon^{1/2}\sqrt{\frac{\eta}{D_f c_1}}\right)^{-1} - 1\right] e^{\varepsilon^{-1}\sqrt{c_1}(\theta - \theta_{r_1})}, \tag{S18}$$

Centre-Composite:

$$f_{0_{centre-comp}}(\theta) = \frac{c_2}{c_1}\left(1 + \varepsilon^{1/2}\sqrt{\frac{\eta}{D_f c_1}}\right)^{-1} e^{-\varepsilon^{-1/2}\sqrt{\frac{\eta}{D_f}}(\theta - \theta_{r_1})} + \frac{\bar{c}_2}{\bar{c}_1}\left(1 + \varepsilon^{1/2}\sqrt{\frac{\eta}{D_f \bar{c}_1}}\right)^{-1} e^{\varepsilon^{-1/2}\sqrt{\frac{\eta}{D_f}}(\theta - \theta_{r_2})}, \tag{S19}$$

Right-Composite:

$$f_{0_{right-comp}}(\theta) = \frac{\alpha B_3 \theta e^{-b_3\theta}}{\beta B_2 e^{-b_2\theta}} + \frac{\bar{c}_2}{\bar{c}_1}\left[\left(1 + \varepsilon^{1/2}\sqrt{\frac{\eta}{D_f \bar{c}_1}}\right)^{-1} - 1\right] e^{-\varepsilon^{-1}\sqrt{\bar{c}_1}(\theta - \theta_{r_2})}, \tag{S20}$$

Maximal Cone Degenerate Patch Left Boundary:

$$\theta_{\text{crit}_1} = \theta_{r_1} + \frac{\varepsilon}{\sqrt{c_1}} \log\left(\left[\left(1+\varepsilon^{1/2}\sqrt{\frac{\eta}{D_f c_1}}\right)^{-1} - 1\right]^{-1}\left(\frac{c_1 f_{\text{crit}}}{c_2} - 1\right)\right), \text{ for } f_{\text{crit}} \geq \frac{c_2}{c_1}\left(1+\varepsilon^{1/2}\sqrt{\frac{\eta}{D_f c_1}}\right)^{-1}, \tag{S21}$$

$$\theta_{\text{crit}_1} = \theta_{r_1} - \varepsilon^{1/2}\sqrt{\frac{D_f}{\eta}} \log\left(\left(1+\varepsilon^{1/2}\sqrt{\frac{\eta}{D_f c_1}}\right)\frac{c_1 f_{\text{crit}}}{c_2}\right), \text{ for } f_{\text{crit}} \leq \frac{c_2}{c_1}\left(1+\varepsilon^{1/2}\sqrt{\frac{\eta}{D_f c_1}}\right)^{-1}, \tag{S22}$$

Minimal Cone Degenerate Patch Right Boundary:

$$\theta_{\text{crit}_2} = \theta_{r_2} + \varepsilon^{1/2}\sqrt{\frac{D_f}{\eta}} \log\left(\left(1+\varepsilon^{1/2}\sqrt{\frac{\eta}{D_f \bar{c}_1}}\right)\frac{\bar{c}_1 f_{\text{crit}}}{\bar{c}_2}\right), \text{ for } f_{\text{crit}} \leq \frac{\bar{c}_2}{\bar{c}_1}\left(1+\varepsilon^{1/2}\sqrt{\frac{\eta}{D_f \bar{c}_1}}\right)^{-1}, \tag{S23}$$

$$\theta_{\text{crit}_2} = \theta_{r_2} - \frac{\varepsilon}{\sqrt{\bar{c}_1}} \log\left(\left[\left(1+\varepsilon^{1/2}\sqrt{\frac{\eta}{D_f \bar{c}_1}}\right)^{-1} - 1\right]^{-1}\left(\frac{\bar{c}_1 f_{\text{crit}}}{\bar{c}_2} - 1\right)\right), \text{ for } f_{\text{crit}} \geq \frac{\bar{c}_2}{\bar{c}_1}\left(1+\varepsilon^{1/2}\sqrt{\frac{\eta}{D_f \bar{c}_1}}\right)^{-1}, \tag{S24}$$

where the maximal and minimal labels above are the other way around to those in the rod loss only cases (which estimate maximal cone degenerate patch width), since here, for the rod and cone loss case, we are estimating the minimal cone degenerate patch width,

- when $f_{\text{crit}} \geq \frac{c_2}{c_1}\left(1+\varepsilon^{1/2}\sqrt{\frac{\eta}{D_f c_1}}\right)^{-1}$, $\theta_{\text{crit}_1} \leq \theta_{r_1}$;
- when $f_{\text{crit}} < \frac{c_2}{c_1}\left(1+\varepsilon^{1/2}\sqrt{\frac{\eta}{D_f c_1}}\right)^{-1}$, $\theta_{\text{crit}_1} > \theta_{r_1}$;
- when $f_{\text{crit}} \geq \frac{\bar{c}_2}{\bar{c}_1}\left(1+\varepsilon^{1/2}\sqrt{\frac{\eta}{D_f \bar{c}_1}}\right)^{-1}$, $\theta_{\text{crit}_2} \geq \theta_{r_2}$;
- when $f_{\text{crit}} < \frac{\bar{c}_2}{\bar{c}_1}\left(1+\varepsilon^{1/2}\sqrt{\frac{\eta}{D_f \bar{c}_1}}\right)^{-1}$, $\theta_{\text{crit}_2} < \theta_{r_2}$.

S2.3 St-st Case 4: narrow patch of rod and cone loss without treatment

As in Section S2.1 there is no centre-outer region, and the left-centre-inner and right-centre-inner regions coalesce into a single centre-inner region (see Fig. A.1(d)).

Left- and Right-Outer:

$$f_0(\theta) = \frac{\alpha B_3 \theta e^{-b_3\theta}}{\beta B_2 e^{-b_2\theta}}, \tag{S25}$$

Left-Inner:

$$f_0(\theta) = A_1 e^{\varepsilon^{-1}\sqrt{c_1}(\theta-\theta_{r_1})} + \frac{c_2}{c_1}, \tag{S26}$$

Centre-Inner:

$$f_0(\theta) = A_3 e^{-\varepsilon^{-1/2}\sqrt{\frac{\eta}{D_f}}(\theta-\theta_{r_1})} + A_4 e^{\varepsilon^{-1/2}\sqrt{\frac{\eta}{D_f}}(\theta-\theta_{r_2})}, \tag{S27}$$

Right-Inner:

$$f_0(\theta) = A_8 e^{-\varepsilon^{-1}\sqrt{\bar{c}_1}(\theta-\theta_{r_2})} + \frac{\bar{c}_2}{\bar{c}_1}, \tag{S28}$$

where:

$$A_1 = (1+B^{-1}Q)\frac{B^{-1}\bar{Q}M^{-1}\frac{c_2}{c_1}+\frac{\bar{c}_2}{\bar{c}_1}}{\bar{B}M-B^{-1}Q\bar{Q}M^{-1}}+(B^{-1}-1)\frac{c_2}{c_1},$$

$$A_3 = B^{-1}\left[\frac{c_2}{c_1}+Q\frac{B^{-1}\bar{Q}M^{-1}\frac{c_2}{c_1}+\frac{\bar{c}_2}{\bar{c}_1}}{\bar{B}M-B^{-1}Q\bar{Q}M^{-1}}\right],$$

$$A_4 = \frac{B^{-1}\bar{Q}\frac{c_2}{c_1}+M\frac{\bar{c}_2}{\bar{c}_1}}{\bar{B}M-B^{-1}Q\bar{Q}M^{-1}},$$

$$A_8 = (M+B^{-1}QM^{-1})\frac{B^{-1}\bar{Q}M^{-1}\frac{c_2}{c_1}+\frac{\bar{c}_2}{\bar{c}_1}}{\bar{B}M-B^{-1}Q\bar{Q}M^{-1}}+B^{-1}M^{-1}\frac{c_2}{c_1}-\frac{\bar{c}_2}{\bar{c}_1},$$

Left-Composite:

$$f_{0_{left-comp}}(\theta) = \frac{\alpha B_3\theta e^{-b_3\theta}}{\beta B_2 e^{-b_2\theta}}+A_1 e^{\varepsilon^{-1}\sqrt{c_1}(\theta-\theta_{r_1})}, \tag{S29}$$

Centre-Composite is identical with the centre-inner.
Right-Composite:

$$f_{0_{right-comp}}(\theta) = \frac{\alpha B_3\theta e^{-b_3\theta}}{\beta B_2 e^{-b_2\theta}}+A_8 e^{-\varepsilon^{-1}\sqrt{\bar{c}_1}(\theta-\theta_{r_2})}, \tag{S30}$$

Maximal Cone Degenerate Patch Left Boundary:

$$\theta_{\text{crit}_1} = \theta_{r_1}+\frac{\varepsilon}{\sqrt{c_1}}\log\left(A_1^{-1}\left(f_{\text{crit}}-\frac{c_2}{c_1}\right)\right), \text{ for } f_{\text{crit}} \geq A_1+\frac{c_2}{c_1}, \tag{S31}$$

$$f_{\text{crit}} = A_3 e^{-\varepsilon^{-1}\sqrt{c_1}(\theta_{\text{crit}_1}-\theta_{r_1})}+A_4 e^{\varepsilon^{-1}\sqrt{c_1}(\theta_{\text{crit}_1}-\theta_{r_2})}, \text{ for } f_{\text{crit}} \leq A_1+\frac{c_2}{c_1}, \tag{S32}$$

Minimal Cone Degenerate Patch Right Boundary:

$$f_{\text{crit}} = A_3 e^{-\varepsilon^{-1}\sqrt{c_1}(\theta_{\text{crit}_2}-\theta_{r_1})}+A_4 e^{\varepsilon^{-1}\sqrt{c_1}(\theta_{\text{crit}_2}-\theta_{r_2})}, \text{ for } f_{\text{crit}} \leq A_8+\frac{\bar{c}_2}{\bar{c}_1}, \tag{S33}$$

$$\theta_{\text{crit}_2} = \theta_{r_2}-\frac{\varepsilon}{\sqrt{\bar{c}_1}}\log\left(A_8^{-1}\left(f_{\text{crit}}-\frac{\bar{c}_2}{\bar{c}_1}\right)\right), \text{ for } f_{\text{crit}} \geq A_8+\frac{\bar{c}_2}{\bar{c}_1}, \tag{S34}$$

where Eqs. (S32) and (S33) must be solved implicitly for θ_{crit_1} and θ_{crit_2} respectively. The maximal and minimal labels above are the other way around to those in the rod loss only cases (which estimate maximal cone degenerate patch width), since here, for the rod and cone loss case, we are estimating the minimal cone degenerate patch width,

- when $f_{\text{crit}} \geq A_1+\frac{c_2}{c_1}$, $\theta_{\text{crit}_1} \leq \theta_{r_1}$;
- when $f_{\text{crit}} < A_1+\frac{c_2}{c_1}$, $\theta_{\text{crit}_1} > \theta_{r_1}$;
- when $f_{\text{crit}} \geq A_8+\frac{\bar{c}_2}{\bar{c}_1}$, $\theta_{\text{crit}_2} \geq \theta_{r_2}$;
- when $f_{\text{crit}} < A_8+\frac{\bar{c}_2}{\bar{c}_1}$, $\theta_{\text{crit}_2} < \theta_{r_2}$.

S2.4 St-st Case 5: wide patch of rod loss with global treatment

This case is the same as that in Appendix A, except that treatment is applied across the whole domain ($T(\theta)=1$) at rate ξ. Thus, we decompose the domain into the same regions as in the untreated case (see Fig. A.1(a)). We rescale $\xi = \varepsilon^{-2}\xi'$, where $\xi' = O(1)$, here and in Sections S2.5–S2.7, dropping the dash.

Left- and Right-Outer:

$$f_0(\theta) = \frac{\alpha B_3 \theta e^{-b_3\theta} + \xi}{\beta B_2 e^{-b_2\theta}}, \tag{S35}$$

Left-Inner:

$$f_0(\theta) = \frac{c_2}{c_1}\left(1 - \frac{1}{2}e^{\varepsilon^{-1}\sqrt{c_1}(\theta-\theta_{r_1})}\right) + \frac{\xi}{D_f c_1}, \tag{S36}$$

Left-Centre-Inner:

$$f_0(\theta) = \frac{c_2}{2c_1}e^{-\varepsilon^{-1}\sqrt{c_1}(\theta-\theta_{r_1})} + \frac{\xi}{D_f c_1}, \tag{S37}$$

Centre-Outer:

$$f_0(\theta) = \frac{\xi}{\beta B_2 e^{-b_2\theta}}, \tag{S38}$$

Right-Centre-Inner:

$$f_0(\theta) = \frac{\bar{c}_2}{2\bar{c}_1}e^{\varepsilon^{-1}\sqrt{\bar{c}_1}(\theta-\theta_{r_2})} + \frac{\xi}{D_f \bar{c}_1}, \tag{S39}$$

Right-Inner:

$$f_0(\theta) = \frac{\bar{c}_2}{\bar{c}_1}\left(1 - \frac{1}{2}e^{-\varepsilon^{-1}\sqrt{\bar{c}_1}(\theta-\theta_{r_2})}\right) + \frac{\xi}{D_f \bar{c}_1}, \tag{S40}$$

Left-Composite:

$$f_{0_{left-comp}}(\theta) = \frac{\alpha B_3 \theta e^{-b_3\theta} + \xi}{\beta B_2 e^{-b_2\theta}} - \frac{c_2}{2c_1}e^{\varepsilon^{-1}\sqrt{c_1}(\theta-\theta_{r_1})}, \tag{S41}$$

Centre-Composite:

$$f_{0_{centre-comp}}(\theta) = \frac{c_2}{2c_1}e^{-\varepsilon^{-1}\sqrt{c_1}(\theta-\theta_{r_1})} + \frac{\xi}{\beta B_2 e^{-b_2\theta}} + \frac{\bar{c}_2}{2\bar{c}_1}e^{\varepsilon^{-1}\sqrt{\bar{c}_1}(\theta-\theta_{r_2})}, \tag{S42}$$

Right-Composite:

$$f_{0_{right-comp}}(\theta) = \frac{\alpha B_3 \theta e^{-b_3\theta} + \xi}{\beta B_2 e^{-b_2\theta}} - \frac{\bar{c}_2}{2\bar{c}_1}e^{-\varepsilon^{-1}\sqrt{\bar{c}_1}(\theta-\theta_{r_2})}, \tag{S43}$$

Minimal Cone Degenerate Patch Left Boundary:

$$\theta_{\text{crit}_1} = \theta_{r_1} + \text{sgn}\left(f_{\text{crit}} - \frac{c_2}{2c_1} - \frac{\xi}{D_f c_1}\right)\frac{\varepsilon}{\sqrt{c_1}}\log\left(1 - \left|\frac{2c_1 f_{\text{crit}}}{c_2} - \frac{2\xi}{D_f c_2} - 1\right|\right), \tag{S44}$$

Maximal Cone Degenerate Patch Right Boundary:

$$\theta_{\text{crit}_2} = \theta_{r_2} - \text{sgn}\left(f_{\text{crit}} - \frac{\bar{c}_2}{2\bar{c}_1} - \frac{\xi}{D_f \bar{c}_1}\right)\frac{\varepsilon}{\sqrt{\bar{c}_1}}\log\left(1 - \left|\frac{2\bar{c}_1 f_{\text{crit}}}{\bar{c}_2} - \frac{2\xi}{D_f \bar{c}_2} - 1\right|\right), \tag{S45}$$

- when $f_{\text{crit}} \geq c_2/(2c_1) + \xi/(D_f c_1)$, $\theta_{\text{crit}_1} \leq \theta_{r_1}$;
- when $f_{\text{crit}} < c_2/(2c_1) + \xi/(D_f c_1)$, $\theta_{\text{crit}_1} > \theta_{r_1}$;
- when $f_{\text{crit}} \geq \bar{c}_2/(2\bar{c}_1) + \xi/(D_f \bar{c}_1)$, $\theta_{\text{crit}_2} \geq \theta_{r_2}$;
- when $f_{\text{crit}} < \bar{c}_2/(2\bar{c}_1) + \xi/(D_f \bar{c}_1)$, $\theta_{\text{crit}_2} < \theta_{r_2}$.

We calculate the critical treatment rate, ξ_{crit}, as the minimal treatment rate required to prevent cone loss, that is, to keep $f \geq f_{\text{crit}}$ local to the patch of rod loss. The minimum TF concentration is achieved at some θ_{crit} within the interval $\theta_{\text{crit}} \in [\theta_{r_1}, \theta_{r_2}]$. Thus, ξ_{crit} and θ_{crit} can be found by setting $\xi = \xi_{\text{crit}}$ and $\theta = \theta_{\text{crit}}$ in both Eqn. (S42) and in the equation obtained by setting $f'_{0_{centre-comp}}(\theta) = 0$ from Eqn. (S42), to provide,

Critical treatment rate:

$$\xi_{\text{crit}} = \beta B_2 e^{-b_2\theta_{\text{crit}}} \left(f_{\text{crit}} - \frac{c_2}{2c_1} e^{-\varepsilon^{-1}\sqrt{c_1}(\theta_{\text{crit}}-\theta_{r_1})} - \frac{\bar{c}_2}{2\bar{c}_1} e^{\varepsilon^{-1}\sqrt{\bar{c}_1}(\theta_{\text{crit}}-\theta_{r_2})} \right), \tag{S46}$$

Eccentricity of the minimum TF concentration:

$$0 = -\frac{\varepsilon^{-1}c_2}{2\sqrt{c_1}} e^{-\varepsilon^{-1}\sqrt{c_1}(\theta_{\text{crit}}-\theta_{r_1})} + \frac{\xi_{\text{crit}} b_2}{\beta B_2 e^{-b_2\theta_{\text{crit}}}} + \frac{\varepsilon^{-1}\bar{c}_2}{2\sqrt{\bar{c}_1}} e^{\varepsilon^{-1}\sqrt{\bar{c}_1}(\theta_{\text{crit}}-\theta_{r_2})}, \tag{S47}$$

solving Eqs. (S46) and (S47) simultaneously.

S2.5 St-st Case 6: wide patch of rod loss with local treatment

This case is the same as that in Section S2.4, except that treatment is only applied locally, within the degenerate rod patch ($T(\theta) = 1 - F(\theta)$), rather than globally, across the whole domain. We decompose the domain into the same regions as in the untreated and global treatment cases (see Fig. A.1(a)).

Left- and Right-Outer:

$$f_0(\theta) = \frac{\alpha B_3 \theta e^{-b_3\theta}}{\beta B_2 e^{-b_2\theta}}, \tag{S48}$$

Left-Inner:

$$f_0(\theta) = \frac{c_2}{c_1} + \left(\frac{\xi}{2D_f c_1} - \frac{c_2}{2c_1} \right) e^{\varepsilon^{-1}\sqrt{c_1}(\theta-\theta_{r_1})}, \tag{S49}$$

Left-Centre-Inner:

$$f_0(\theta) = \left(\frac{c_2}{2c_1} - \frac{\xi}{2D_f c_1} \right) e^{-\varepsilon^{-1}\sqrt{c_1}(\theta-\theta_{r_1})} + \frac{\xi}{D_f c_1}, \tag{S50}$$

Centre-Outer:

$$f_0(\theta) = \frac{\xi}{\beta B_2 e^{-b_2\theta}}, \tag{S51}$$

Right-Centre-Inner:

$$f_0(\theta) = \left(\frac{\bar{c}_2}{2\bar{c}_1} - \frac{\xi}{2D_f \bar{c}_1} \right) e^{\varepsilon^{-1}\sqrt{\bar{c}_1}(\theta-\theta_{r_2})} + \frac{\xi}{D_f \bar{c}_1}, \tag{S52}$$

Right-Inner:

$$f_0(\theta) = \frac{\bar{c}_2}{\bar{c}_1} + \left(\frac{\xi}{2D_f \bar{c}_1} - \frac{\bar{c}_2}{2\bar{c}_1} \right) e^{-\varepsilon^{-1}\sqrt{\bar{c}_1}(\theta-\theta_{r_2})}, \tag{S53}$$

Left-Composite:

$$f_{0_{left-comp}}(\theta) = \frac{\alpha B_3 \theta e^{-b_3\theta}}{\beta B_2 e^{-b_2\theta}} + \left(\frac{\xi}{2D_f c_1} - \frac{c_2}{2c_1} \right) e^{\varepsilon^{-1}\sqrt{c_1}(\theta-\theta_{r_1})}, \tag{S54}$$

Centre-Composite:

$$f_{0_{centre-comp}}(\theta) = \left(\frac{c_2}{2c_1} - \frac{\xi}{2D_f c_1} \right) e^{-\varepsilon^{-1}\sqrt{c_1}(\theta-\theta_{r_1})} + \frac{\xi}{\beta B_2 e^{-b_2\theta}} + \left(\frac{\bar{c}_2}{2\bar{c}_1} - \frac{\xi}{2D_f \bar{c}_1} \right) e^{\varepsilon^{-1}\sqrt{\bar{c}_1}(\theta-\theta_{r_2})}, \tag{S55}$$

Right-Composite:

$$f_{0_{right-comp}}(\theta) = \frac{\alpha B_3 \theta e^{-b_3\theta}}{\beta B_2 e^{-b_2\theta}} + \left(\frac{\xi}{2D_f \bar{c}_1} - \frac{\bar{c}_2}{2\bar{c}_1} \right) e^{-\varepsilon^{-1}\sqrt{\bar{c}_1}(\theta-\theta_{r_2})}, \tag{S56}$$

Minimal Cone Degenerate Patch Left Boundary:

$$\theta_{\text{crit}_1} = \theta_{r_1} + \text{sgn}\left(f_{\text{crit}} - \frac{c_2}{2c_1} - \frac{\xi}{2D_f c_1}\right)\frac{\varepsilon}{\sqrt{c_1}}\log\left(\left(1-\frac{\xi}{D_f c_2}\right)^{-1}\left(1-\frac{\xi}{D_f c_2} - \left|\frac{2c_1 f_{\text{crit}}}{c_2} - 1 - \frac{\xi}{D_f c_2}\right|\right)\right), \quad \text{(S57)}$$

Maximal Cone Degenerate Patch Right Boundary:

$$\theta_{\text{crit}_2} = \theta_{r_2} - \text{sgn}\left(f_{\text{crit}} - \frac{\bar{c}_2}{2\bar{c}_1} - \frac{\xi}{2D_f \bar{c}_1}\right)\frac{\varepsilon}{\sqrt{\bar{c}_1}}\log\left(\left(1-\frac{\xi}{D_f \bar{c}_2}\right)^{-1}\left(1-\frac{\xi}{D_f \bar{c}_2} - \left|\frac{2\bar{c}_1 f_{\text{crit}}}{\bar{c}_2} - 1 - \frac{\xi}{D_f c_2}\right|\right)\right), \quad \text{(S58)}$$

- when $f_{\text{crit}} \geq c_2/(2c_1) + \xi/(2D_f c_1)$, $\theta_{\text{crit}_1} \leq \theta_{r_1}$;
- when $f_{\text{crit}} < c_2/(2c_1) + \xi/(2D_f c_1)$, $\theta_{\text{crit}_1} > \theta_{r_1}$;
- when $f_{\text{crit}} \geq \bar{c}_2/(2\bar{c}_1) + \xi/(2D_f \bar{c}_1)$, $\theta_{\text{crit}_2} \geq \theta_{r_2}$;
- when $f_{\text{crit}} < \bar{c}_2/(2\bar{c}_1) + \xi/(2D_f \bar{c}_1)$, $\theta_{\text{crit}_2} < \theta_{r_2}$.

Critical treatment rate:

$$\begin{aligned}\xi_{\text{crit}} = &\left(f_{\text{crit}} - \frac{c_2}{2c_1}e^{-\varepsilon^{-1}\sqrt{c_1}(\theta_{\text{crit}}-\theta_{r_1})} - \frac{\bar{c}_2}{2\bar{c}_1}e^{\varepsilon^{-1}\sqrt{\bar{c}_1}(\theta_{\text{crit}}-\theta_{r_2})}\right)\times \\ &\left(\frac{1}{\beta B_2 e^{-b_2\theta_{\text{crit}}}} - \frac{1}{2D_f c_1}e^{-\varepsilon^{-1}\sqrt{c_1}(\theta_{\text{crit}}-\theta_{r_1})} - \frac{1}{2D_f \bar{c}_1}e^{\varepsilon^{-1}\sqrt{\bar{c}_1}(\theta_{\text{crit}}-\theta_{r_2})}\right)^{-1}, \quad \text{(S59)}\end{aligned}$$

Eccentricity of the minimum TF concentration:

$$0 = -\varepsilon^{-1}\sqrt{c_1}\left(\frac{c_2}{2c_1} - \frac{\xi_{\text{crit}}}{2D_f c_1}\right)e^{-\varepsilon^{-1}\sqrt{c_1}(\theta_{\text{crit}}-\theta_{r_1})} + \frac{\xi_{\text{crit}} b_2}{\beta B_2 e^{-b_2\theta_{\text{crit}}}} + \varepsilon^{-1}\sqrt{\bar{c}_1}\left(\frac{\bar{c}_2}{2\bar{c}_1} - \frac{\xi_{\text{crit}}}{2D_f \bar{c}_1}\right)e^{\varepsilon^{-1}\sqrt{\bar{c}_1}(\theta_{\text{crit}}-\theta_{r_2})}, \quad \text{(S60)}$$

solving Eqs. (S59) and (S60) simultaneously for ξ_{crit} and θ_{crit}.

S2.6 St-st Case 7: narrow patch of rod loss with global treatment

This case is the same as that in Section S2.1, except that treatment is applied across the whole domain ($T(\theta) = 1$) at rate ξ. Thus, we decompose the domain into the same regions as in the untreated case (see Fig. A.1(b)).

Left- and Right-Outer:

$$f_0(\theta) = \frac{\alpha B_3 \theta e^{-b_3\theta} + \xi}{\beta B_2 e^{-b_2\theta}}, \quad \text{(S61)}$$

Left-Inner:

$$f_0(\theta) = A_1 e^{\varepsilon^{-1}\sqrt{c_1}(\theta-\theta_{r_1})} + \frac{c_2}{c_1} + \frac{\xi}{D_f c_1}, \quad \text{(S62)}$$

Centre-Inner:

$$f_0(\theta) = A_3 e^{-\varepsilon^{-1}\sqrt{c_1}(\theta-\theta_{r_1})} + A_4 e^{\varepsilon^{-1}\sqrt{c_1}(\theta-\theta_{r_2})} + \frac{\xi}{D_f c_1}, \quad \text{(S63)}$$

Right-Inner:

$$f_0(\theta) = A_8 e^{-\varepsilon^{-1}\sqrt{\bar{c}_1}(\theta-\theta_{r_2})} + \frac{\bar{c}_2}{\bar{c}_1} + \frac{\xi}{D_f \bar{c}_1}, \quad \text{(S64)}$$

where:

$$A_1 = \left(1+\sqrt{\frac{c_1}{\bar{c}_1}}\right)^{-1}\left[\frac{c_2}{2c_1}K^{-2}\left(\sqrt{\frac{c_1}{\bar{c}_1}}-1\right)+K^{-1}\left(\frac{\bar{c}_2}{\bar{c}_1}+\frac{\xi}{D_f\bar{c}_1}-\frac{\xi}{D_f c_1}\right)\right]-\frac{c_2}{2c_1},$$
$$A_3 = \frac{c_2}{2c_1},$$
$$A_4 = \left(1+\sqrt{\frac{c_1}{\bar{c}_1}}\right)^{-1}\left[\frac{c_2}{2c_1}K^{-1}\left(\sqrt{\frac{c_1}{\bar{c}_1}}-1\right)+\left(\frac{\bar{c}_2}{\bar{c}_1}+\frac{\xi}{D_f\bar{c}_1}-\frac{\xi}{D_f c_1}\right)\right],$$
$$A_8 = -\left(1+\sqrt{\frac{c_1}{\bar{c}_1}}\right)^{-1}\left[\frac{c_2}{2c_1}K^{-1}\left(\sqrt{\frac{c_1}{\bar{c}_1}}-1\right)+\left(\frac{\bar{c}_2}{\bar{c}_1}+\frac{\xi}{D_f\bar{c}_1}-\frac{\xi}{D_f c_1}\right)\right]\sqrt{\frac{c_1}{\bar{c}_1}}+\frac{c_2}{2c_1}\sqrt{\frac{c_1}{\bar{c}_1}}K^{-1},$$

Left-Composite:

$$f_{0_{left-comp}}(\theta) = \frac{\alpha B_3\theta e^{-b_3\theta}+\xi}{\beta B_2 e^{-b_2\theta}}+A_1 e^{\varepsilon^{-1}\sqrt{c_1}(\theta-\theta_{r_1})}, \tag{S65}$$

Centre-Composite is identical with the centre-inner.
Right-Composite:

$$f_{0_{right-comp}}(\theta) = \frac{\alpha B_3\theta e^{-b_3\theta}+\xi}{\beta B_2 e^{-b_2\theta}}+A_8 e^{-\varepsilon^{-1}\sqrt{\bar{c}_1}(\theta-\theta_{r_2})}, \tag{S66}$$

Minimal Cone Degenerate Patch Left Boundary:

$$\theta_{\text{crit}_1} = \theta_{r_1}+\frac{\varepsilon}{\sqrt{c_1}}\log\left(A_1^{-1}\left(f_{\text{crit}}-\frac{c_2}{c_1}-\frac{\xi}{D_f c_1}\right)\right), \text{ for } f_{\text{crit}} \geq A_1+\frac{c_2}{c_1}+\frac{\xi}{D_f c_1}, \tag{S67}$$
$$f_{\text{crit}} = A_3 e^{-\varepsilon^{-1}\sqrt{c_1}(\theta_{\text{crit}_1}-\theta_{r_1})}+A_4 e^{\varepsilon^{-1}\sqrt{c_1}(\theta_{\text{crit}_1}-\theta_{r_2})}+\frac{\xi}{D_f c_1}, \text{ for } f_{\text{crit}} \leq A_1+\frac{c_2}{c_1}+\frac{\xi}{D_f c_1}, \tag{S68}$$

Maximal Cone Degenerate Patch Right Boundary:

$$f_{\text{crit}} = A_3 e^{-\varepsilon^{-1}\sqrt{c_1}(\theta_{\text{crit}_2}-\theta_{r_1})}+A_4 e^{\varepsilon^{-1}\sqrt{c_1}(\theta_{\text{crit}_2}-\theta_{r_2})}+\frac{\xi}{D_f c_1}, \text{ for } f_{\text{crit}} \leq A_8+\frac{\bar{c}_2}{\bar{c}_1}+\frac{\xi}{D_f\bar{c}_1}, \tag{S69}$$
$$\theta_{\text{crit}_2} = \theta_{r_2}-\frac{\varepsilon}{\sqrt{\bar{c}_1}}\log\left(A_8^{-1}\left(f_{\text{crit}}-\frac{\bar{c}_2}{\bar{c}_1}-\frac{\xi}{D_f\bar{c}_1}\right)\right), \text{ for } f_{\text{crit}} \geq A_8+\frac{\bar{c}_2}{\bar{c}_1}+\frac{\xi}{D_f\bar{c}_1}, \tag{S70}$$

where Eqs. (S68) and (S69) must be solved implicitly for θ_{crit_1} and θ_{crit_2} respectively,

- when $f_{\text{crit}} \geq A_1+\frac{c_2}{c_1}+\frac{\xi}{D_f c_1}$, $\theta_{\text{crit}_1} \leq \theta_{r_1}$;
- when $f_{\text{crit}} < A_1+\frac{c_2}{c_1}+\frac{\xi}{D_f c_1}$, $\theta_{\text{crit}_1} > \theta_{r_1}$;
- when $f_{\text{crit}} \geq A_8+\frac{\bar{c}_2}{\bar{c}_1}+\frac{\xi}{D_f\bar{c}_1}$, $\theta_{\text{crit}_2} \geq \theta_{r_2}$;
- when $f_{\text{crit}} < A_8+\frac{\bar{c}_2}{\bar{c}_1}+\frac{\xi}{D_f\bar{c}_1}$, $\theta_{\text{crit}_2} < \theta_{r_2}$.

Critical treatment rate:

$$\xi_{\text{crit}} = \left(f_{\text{crit}}-\left(1+\sqrt{\frac{c_1}{\bar{c}_1}}\right)^{-1}\left[\frac{c_2}{2c_1}K^{-2}\left(\sqrt{\frac{c_1}{\bar{c}_1}}-1\right)+K^{-1}\frac{\bar{c}_2}{\bar{c}_1}\right]e^{\varepsilon^{-1}\sqrt{c_1}(\theta_{\text{crit}}-\theta_{r_1})}-\frac{c_2}{2c_1}e^{-\varepsilon^{-1}\sqrt{c_1}(\theta_{\text{crit}}-\theta_{r_1})}\right)\times$$
$$\left(\frac{1}{D_f c_1}+\left(1+\sqrt{\frac{c_1}{\bar{c}_1}}\right)^{-1}K^{-1}\left(\frac{1}{D_f\bar{c}_1}-\frac{1}{D_f c_1}\right)e^{\varepsilon^{-1}\sqrt{c_1}(\theta_{\text{crit}}-\theta_{r_1})}\right)^{-1}, \tag{S71}$$

Eccentricity of the minimum TF concentration:

$$\theta_{\text{crit}} = \theta_{r_1} - \frac{\varepsilon}{2\sqrt{c_1}} \log\left(\frac{2c_1}{c_2} \left(1 + \sqrt{\frac{c_1}{\bar{c}_1}}\right)^{-1} \left[\frac{c_2}{2c_1} K^{-2} \left(\sqrt{\frac{c_1}{\bar{c}_1}} - 1 \right) + K^{-1} \left(\frac{\bar{c}_2}{\bar{c}_1} + \frac{\xi_{\text{crit}}}{D_f \bar{c}_1} - \frac{\xi_{\text{crit}}}{D_f c_1} \right) \right] \right), \tag{S72}$$

solving Eqs. (S71) and (S72) simultaneously for ξ_{crit} and θ_{crit}.

S2.7 St-st Case 8: narrow patch of rod loss with local treatment

This case is the same as that in Section S2.6, except that treatment is only applied locally, within the degenerate rod patch ($T(\theta) = 1 - F(\theta)$), rather than globally, across the whole domain. We decompose the domain into the same regions as in the untreated and global treatment cases (see Fig. A.1(b)).

Left- and Right-Outer:

$$f_0(\theta) = \frac{\alpha B_3 \theta e^{-b_3 \theta}}{\beta B_2 e^{-b_2 \theta}}, \tag{S73}$$

Left-Inner:

$$f_0(\theta) = A_1 e^{\varepsilon^{-1}\sqrt{c_1}(\theta - \theta_{r_1})} + \frac{c_2}{c_1}, \tag{S74}$$

Centre-Inner:

$$f_0(\theta) = A_3 e^{-\varepsilon^{-1}\sqrt{c_1}(\theta - \theta_{r_1})} + A_4 e^{\varepsilon^{-1}\sqrt{c_1}(\theta - \theta_{r_2})} + \frac{\xi}{D_f c_1}, \tag{S75}$$

Right-Inner:

$$f_0(\theta) = A_8 e^{-\varepsilon^{-1}\sqrt{\bar{c}_1}(\theta - \theta_{r_2})} + \frac{\bar{c}_2}{\bar{c}_1}, \tag{S76}$$

where:

$$A_1 = \left(1 + \sqrt{\frac{c_1}{\bar{c}_1}}\right)^{-1} \left[\frac{K^{-2}}{2} \left(\frac{c_2}{c_1} - \frac{\xi}{D_f c_1} \right) \left(\sqrt{\frac{c_1}{\bar{c}_1}} - 1 \right) + K^{-1} \left(\frac{\bar{c}_2}{\bar{c}_1} - \frac{\xi}{D_f c_1} \right) \right] - \frac{1}{2} \left(\frac{c_2}{c_1} - \frac{\xi}{D_f c_1} \right),$$

$$A_3 = \frac{1}{2} \left(\frac{c_2}{c_1} - \frac{\xi}{D_f c_1} \right),$$

$$A_4 = \left(1 + \sqrt{\frac{c_1}{\bar{c}_1}}\right)^{-1} \left[\frac{K^{-1}}{2} \left(\frac{c_2}{c_1} - \frac{\xi}{D_f c_1} \right) \left(\sqrt{\frac{c_1}{\bar{c}_1}} - 1 \right) + \left(\frac{\bar{c}_2}{\bar{c}_1} - \frac{\xi}{D_f c_1} \right) \right],$$

$$A_8 = -\left(1 + \sqrt{\frac{c_1}{\bar{c}_1}}\right)^{-1} \left[\frac{K^{-1}}{2} \left(\frac{c_2}{c_1} - \frac{\xi}{D_f c_1} \right) \left(\sqrt{\frac{c_1}{\bar{c}_1}} - 1 \right) + \left(\frac{\bar{c}_2}{\bar{c}_1} - \frac{\xi}{D_f c_1} \right) \right] \sqrt{\frac{c_1}{\bar{c}_1}} + \sqrt{\frac{c_1}{\bar{c}_1}} \frac{K^{-1}}{2} \left(\frac{c_2}{c_1} - \frac{\xi}{D_f c_1} \right),$$

Left-Composite:

$$f_{0_{left-comp}}(\theta) = \frac{\alpha B_3 \theta e^{-b_3 \theta}}{\beta B_2 e^{-b_2 \theta}} + A_1 e^{\varepsilon^{-1}\sqrt{c_1}(\theta - \theta_{r_1})}, \tag{S77}$$

Centre-Composite is identical with the centre-inner.
Right-Composite:

$$f_{0_{right-comp}}(\theta) = \frac{\alpha B_3 \theta e^{-b_3 \theta}}{\beta B_2 e^{-b_2 \theta}} + A_8 e^{-\varepsilon^{-1}\sqrt{\bar{c}_1}(\theta - \theta_{r_2})}, \tag{S78}$$

The Left- and Right-Composite solutions are the same here as for the narrow patch without treatment (Eqs. (S5) and (S6)), except that the expressions for A_1 and A_8 are different.
Minimal Cone Degenerate Patch Left Boundary:

$$\theta_{\text{crit}_1} = \theta_{r_1} + \frac{\varepsilon}{\sqrt{c_1}} \log\left(A_1^{-1} \left(f_{\text{crit}} - \frac{c_2}{c_1} \right) \right), \text{ for } f_{\text{crit}} \geq A_1 + \frac{c_2}{c_1}, \tag{S79}$$

$$f_{\text{crit}} = A_3 e^{-\varepsilon^{-1}\sqrt{c_1}(\theta_{\text{crit}_1} - \theta_{r_1})} + A_4 e^{\varepsilon^{-1}\sqrt{c_1}(\theta_{\text{crit}_1} - \theta_{r_2})}, \text{ for } f_{\text{crit}} \leq A_1 + \frac{c_2}{c_1}, \tag{S80}$$

Maximal Cone Degenerate Patch Right Boundary:

$$f_{\text{crit}} = A_3 e^{-\varepsilon^{-1}\sqrt{c_1}(\theta_{\text{crit}_2}-\theta_{r_1})} + A_4 e^{\varepsilon^{-1}\sqrt{c_1}(\theta_{\text{crit}_2}-\theta_{r_2})}, \text{ for } f_{\text{crit}} \leq A_8 + \frac{\bar{c}_2}{\bar{c}_1}, \tag{S81}$$

$$\theta_{\text{crit}_2} = \theta_{r_2} - \frac{\varepsilon}{\sqrt{\bar{c}_1}} \log\left(A_8^{-1}\left(f_{\text{crit}} - \frac{\bar{c}_2}{\bar{c}_1}\right)\right), \text{ for } f_{\text{crit}} \geq A_8 + \frac{\bar{c}_2}{\bar{c}_1}, \tag{S82}$$

where Eqs. (S80) and (S81) must be solved implicitly for θ_{crit_1} and θ_{crit_2} respectively,

- when $f_{\text{crit}} \geq A_1 + \frac{c_2}{c_1}$, $\theta_{\text{crit}_1} \leq \theta_{r_1}$;
- when $f_{\text{crit}} < A_1 + \frac{c_2}{c_1}$, $\theta_{\text{crit}_1} > \theta_{r_1}$;
- when $f_{\text{crit}} \geq A_8 + \frac{\bar{c}_2}{\bar{c}_1}$, $\theta_{\text{crit}_2} \geq \theta_{r_2}$;
- when $f_{\text{crit}} < A_8 + \frac{\bar{c}_2}{\bar{c}_1}$, $\theta_{\text{crit}_2} < \theta_{r_2}$.

Critical treatment rate:

$$\xi_{\text{crit}} = \left(f_{\text{crit}} - \left(1+\sqrt{\frac{c_1}{\bar{c}_1}}\right)^{-1}\left[\frac{c_2}{2c_1}K^{-2}\left(\sqrt{\frac{c_1}{\bar{c}_1}}-1\right)+K^{-1}\frac{\bar{c}_2}{\bar{c}_1}\right]e^{\varepsilon^{-1}\sqrt{c_1}(\theta_{\text{crit}}-\theta_{r_1})} - \frac{c_2}{2c_1}e^{-\varepsilon^{-1}\sqrt{c_1}(\theta_{\text{crit}}-\theta_{r_1})}\right) \times$$
$$\left(\left(1+\sqrt{\frac{c_1}{\bar{c}_1}}\right)^{-1}\left[-\left(\sqrt{\frac{c_1}{\bar{c}_1}}-1\right)\frac{K^{-2}}{2D_f c_1} - \frac{K^{-1}}{D_f c_1}\right]e^{\varepsilon^{-1}\sqrt{c_1}(\theta_{\text{crit}}-\theta_{r_1})} - \frac{1}{2D_f c_1}e^{-\varepsilon^{-1}\sqrt{c_1}(\theta_{\text{crit}}-\theta_{r_1})} + \frac{1}{D_f c_1}\right)^{-1}, \tag{S83}$$

Eccentricity of the minimum TF concentration:

$$\theta_{\text{crit}} = \theta_{r_1} - \frac{\varepsilon}{2\sqrt{c_1}}\log\left(2\left(\frac{c_2}{c_1}-\frac{\xi_{\text{crit}}}{D_f c_1}\right)^{-1}\left(1+\sqrt{\frac{c_1}{\bar{c}_1}}\right)^{-1}\left[\left(\frac{c_2}{c_1}-\frac{\xi_{\text{crit}}}{D_f c_1}\right)\frac{K^{-2}}{2}\left(\sqrt{\frac{c_1}{\bar{c}_1}}-1\right)+K^{-1}\left(\frac{\bar{c}_2}{\bar{c}_1}-\frac{\xi_{\text{crit}}}{D_f c_1}\right)\right]\right), \tag{S84}$$

solving Eqs. (S83) and (S84) simultaneously for ξ_{crit} and θ_{crit}.

S3 Supplementary figures

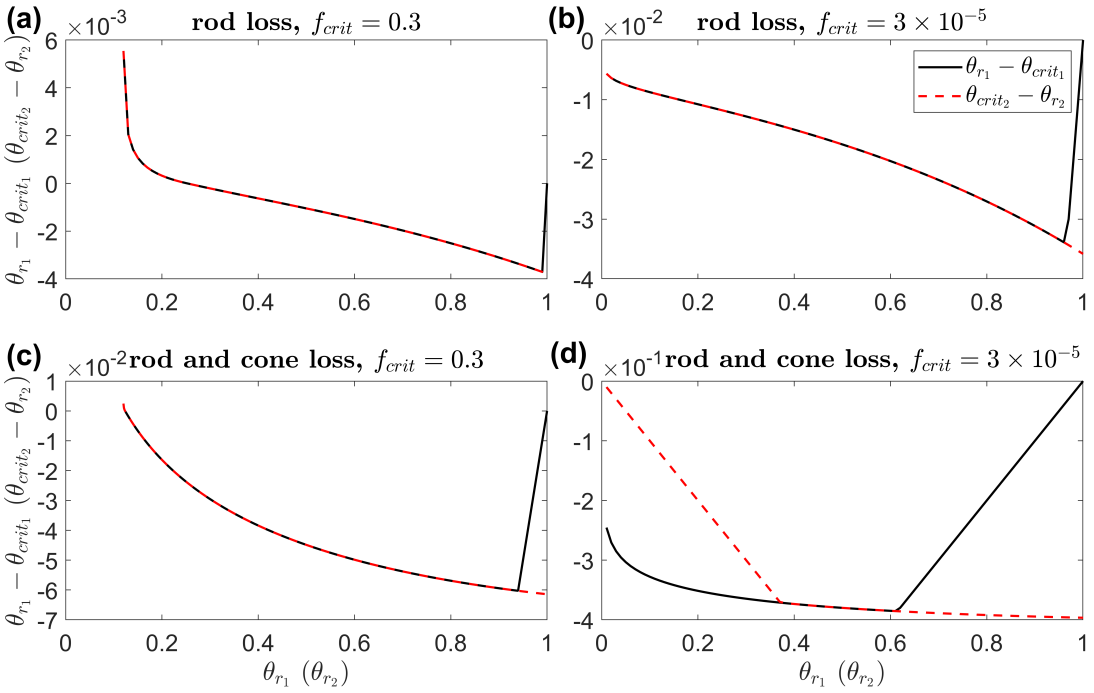

Figure S2: Distance between rod and minimum/maximum cone degenerate patch boundaries using the steady-state model — wide rod degenerate patch (St-st Cases 1 and 3). Each panel shows the variation in the distances between the left-hand rod and minimum cone degenerate patch boundaries, $\theta_{r_1} - \theta_{\text{crit}_1}$, and between the right-hand rod and maximum cone degenerate patch boundaries, $\theta_{\text{crit}_2} - \theta_{r_2}$, with θ_{r_1} and θ_{r_2} respectively. (a) St-st Case 1(ii): rod loss only with $f_{\text{crit}} = 0.3$; (b) St-st Case 1(i): rod loss only with $f_{\text{crit}} = 3 \times 10^{-5}$; (c) St-st Case 3(ii): rod and cone loss with $f_{\text{crit}} = 0.3$; (d) St-st Case 3(i): rod and cone loss with $f_{\text{crit}} = 3 \times 10^{-5}$. Note the different scales on the y-axes. The maximum spatial extent of cone loss remains within the boundaries of rod loss in (b) and (d), but may exceed it close to the fovea (centred at $\theta = 0$) in (a) and (c). Curves are plotted using Eqs. A.22 and A.23 in (a) and (b), and using Eqs. (S21)–(S24) in (c) and (d). The parameter $\varepsilon = 10^{-2}$. Remaining parameter values as in Table 2.

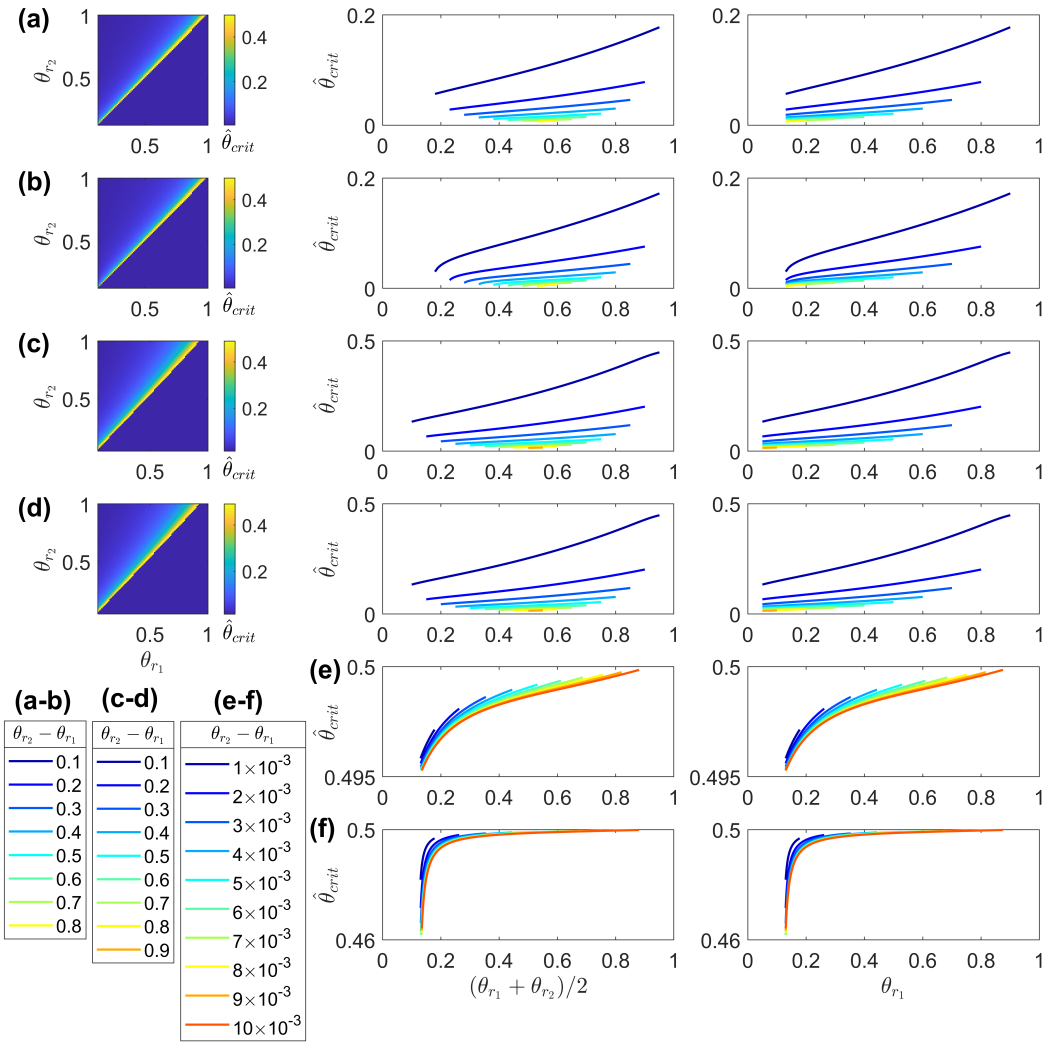

Figure S3: Analytical estimates of the eccentricity of the minimum TF concentration using the steady-state model — wide and narrow rod degenerate patch with rod loss only (St-st Cases 5–8). All plots show the normalised eccentricity of the minimum TF concentration, $\hat{\theta}_{\text{crit}} = (\theta_{\text{crit}} - \theta_{r_1})/(\theta_{r_2} - \theta_{r_1})$. (a) and (c) St-st Case 5, and (e) St-st Case 7 global treatment; (b) and (d) St-st Case 6, and (f) St-st Case 8 local treatment; (a)–(d) wide patch; (e) and (f) narrow patch; (a), (b), (e) and (f) Subcase (ii): $f_{\text{crit}} = 0.3$; (c) and (d) Subcase (i): $f_{\text{crit}} = 3 \times 10^{-5}$. (a)–(d) column 1: variation in $\hat{\theta}_{\text{crit}}$ over $(\theta_{r_1}, \theta_{r_2})$ parameter space. (a)–(f) column 2: variation in $\hat{\theta}_{\text{crit}}$ with rod degenerate patch centre position, $(\theta_{r_1} + \theta_{r_2})/2$; column 3: variation in $\hat{\theta}_{\text{crit}}$ with rod degenerate patch left boundary position, θ_{r_1}; each curve represents a constant rod degenerate patch width, $\theta_{r_2} - \theta_{r_1}$. $\hat{\theta}_{\text{crit}}$ increases monotonically with decreasing rod degenerate patch width and with increasing rod degenerate patch centre/left boundary position in all cases. $\hat{\theta}_{\text{crit}}$ remains close to 0 for patches of width $\theta_{r_2} - \theta_{r_1} \geq 0.2$ ((a)–(d)) and close to 0.5 for narrow patches ((e) and (f)). Analytical solutions are obtained by implicitly solving Eqs. (S46) and (S47) in (a) and (c), Eqs. (S59) and (S60) in (b) and (d), Eqs. (S71) and (S72) in (e), and Eqs. (S83) and (S84) in (f). The parameter $\varepsilon = 10^{-2}$. Remaining parameter values as in Table 2.

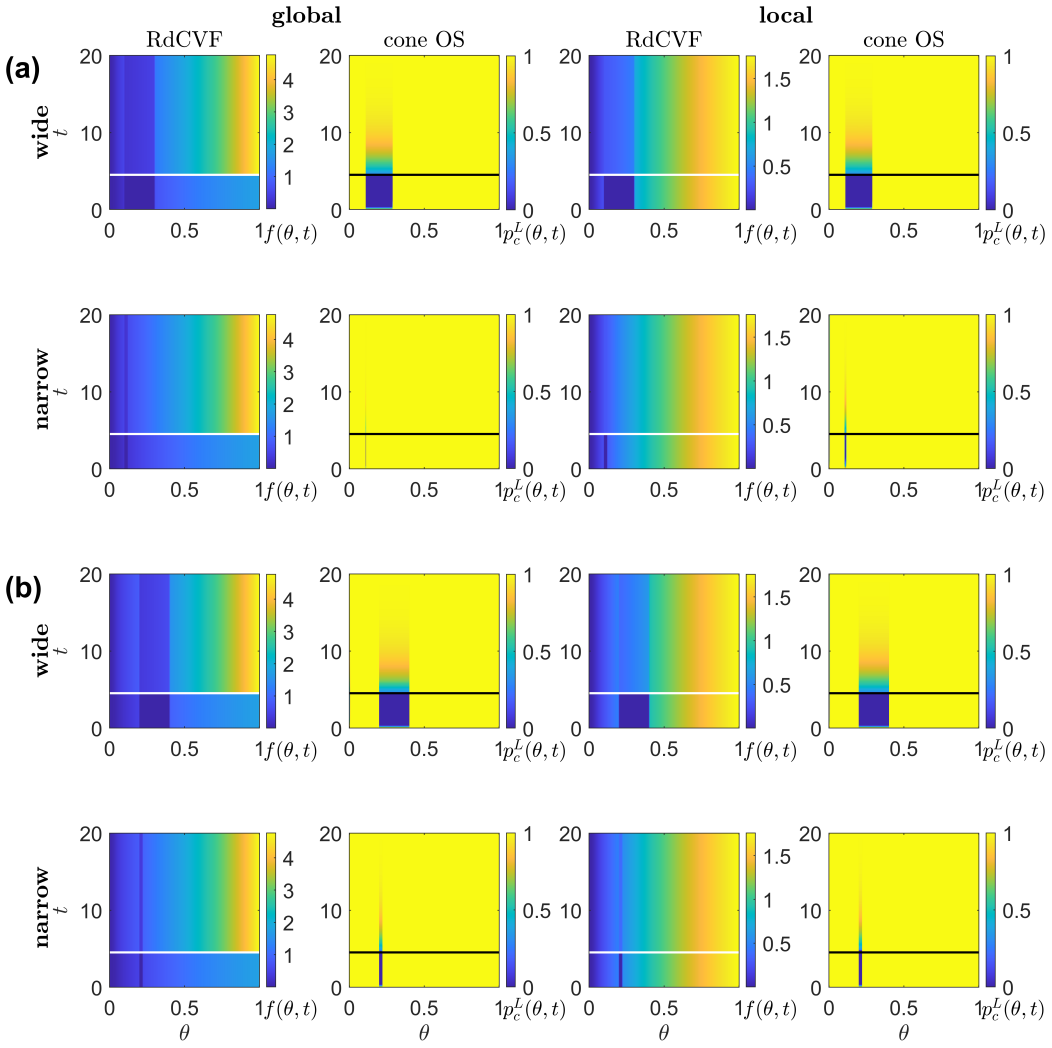

Figure S4: Simulations of the effects of treatment upon RdCVF and cone OS dynamics following the complete removal of rods from the interval $(\theta_{r_1},\theta_{r_2})$ — dynamic model (Dyn Case 4). Panels show TF concentration, $f(\theta,t)$, and cone OS length, $p_c^L(\theta,t)$, for global treatment (columns 1 and 2), $T(\theta,t)=H(t-t_{\text{crit}})$, and local treatment (columns 3 and 4), $T(\theta,t)=(1-F(\theta))H(t-t_{\text{crit}})$, following the removal of rods from wide (width $O(1)$) patches (rows 1 and 3), (a) $(\theta_{r_1},\theta_{r_2})=(0.1,0.3)$ and (b) $(\theta_{r_1},\theta_{r_2})=(0.2,0.4)$, and narrow (width $O(\varepsilon)$) patches (rows 2 and 4), (a) $(\theta_{r_1},\theta_{r_2})=(0.1,0.12)$ and (b) $(\theta_{r_1},\theta_{r_2})=(0.2,0.22)$. Black and white horizontal lines mark the time point, t_{crit}, at which treatment is introduced. (a) Dyn Case 4(i): $f_{\text{crit}}=3\times10^{-5}$; (b) Dyn Case 4(ii): $f_{\text{crit}}=0.3$. All simulations span the period of $\sim$2.2 years in dimensional variables. Treatment results in the complete recovery of cone OSs in all cases. Eqs. (7), (8) and (10)–(12) were solved using the method of lines, with 401 mesh points, $F(\theta)=H(\theta_{r_1}-\theta)+H(\theta-\theta_{r_2})$ and $G(\theta)=1$, and without mutation-induced rod degeneration. Parameter values: $\xi=6\times10^4$ and $t_{\text{crit}}=4.53$ (=1 year in dimensional variables). Remaining parameter values as in Table 2.

References

Chalmel, F., Léveillard, T., Jaillard, C., Lardenois, A., Berdugo, N., Morel, E., Koehl, P., Lambrou, G., Holmgren, A., Sahel, J.A., Poch, O., 2007. Rod-derived cone viability factor-2 is a novel bifunctional-thioredoxin-like protein with therapeutic potential. BMC Molecular Biol. 8. doi:https://doi.org/10.1186/1471-2199-8-74.

Curcio, C.A., Millican, C.L., Allen, K.A., Kalina, R.E., 1993. Aging of the human photoreceptor mosaic: evidence for selective vulnerability of rods in central retina. Invest. Ophthalmol. Vis. Sci. 34, 3278–3296.

Curcio, C.A., Sloan, K.R., Kalina, R.E., Hendrickson, A.E., 1990. Human photoreceptor topography. J. Comp. Neurol. 292, 497–523. doi:https://doi.org/10.1002/cne.902920402.

Dörrbaum, A.R., Kochen, L., Langer, J.D., Schuman, E.M., 2018. Local and global influences on protein turnover in neurons and glia. eLife 7, e34202. doi:10.7554/eLife.34202.

Eden, E., Geva-Zatorsky, N., Issaeva, I., Cohen, A., Dekel, E., Danon, T., Cohen, L., Mayo, A., Alon, U., 2011. Proteome half-life dynamics in living human cells. Science 331, 764–768. doi:10.1126/science.1199784.

Guérin, C.J., Lewis, G.P., Fisher, S.K., Anderson, D.H., 1993. Recovery of photoreceptor outer segment length and analysis of membrane assembly rates in regenerating primate photoreceptor outer segments. Invest. Ophthalmol. Vis. Sci. 34, 175–183.

Jonnal, R.S., Besecker, J.R., Derby, J.C., Kocaoglu, O.P., Cense, B., Gao, W., Wang, Q., Miller, D.T., 2010. Imaging outer segment renewal in living human cone photoreceptors. Opt. Express 18, 5257–5270. doi:https://doi.org/10.1364/OE.18.005257.

Jonnal, R.S., Kocaoglu, O.P., Wang, Q., Lee, S., Miller, D.T., 2012. Phase-sensitive imaging of the outer retina using optical coherence tomography and adaptive optics. Biomed. Opt. Express 3, 104–124. doi:https://doi.org/10.1364/BOE.3.000104.

Jürgens, K.D., Peters, T., Gros, G., 1994. Diffusivity of myoglobin in intact skeletal muscle cells. Proc. Natl. Acad. Sci. 91, 3829–3833. doi:https://doi.org/10.1073/pnas.91.9.3829.

Kocaoglu, O.P., Liu, Z., Zhang, F., Kurokawa, K., Jonnal, R.S., Miller, D.T., 2016. Photoreceptor disc shedding in the living human eye. Biomed. Opt. Express 7, 4554–4568. doi:https://doi.org/10.1364/BOE.7.004554.

Léveillard, T., Mohand-Saïd, S., Lorentz, O., Hicks, D., Fintz, A.C., Clérin, E., Simonutti, M., Forster, V., Cavusoglu, N., Chalmel, F., Dollé, P., Poch, O., Lambrou, G., Sahel, J.A., 2004. Identification and characterization of rod-derived cone viability factor. Nat. Genet. 36, 755–759. doi:https://doi.org/10.1038/ng1386.

McGuire, B.J., Secomb, T.W., 2001. A theoretical model for oxygen transport in skeletal muscle under conditions of high oxygen demand. J. Appl. Physiol. 91, 2255–2265. doi:https://doi.org/10.1152/jappl.2001.91.5.2255.

Oyster, C.W., 1999. The Human Eye: Structure and Function. Sinauer Associates Inc.

Pircher, M., Kroisamer, J.S., Felberer, F., Sattmann, H., Götzinger, E., Hitzenberger, C.K., 2011. Temporal changes of human cone photoreceptors observed in vivo with SLO/OCT. Biomed. Opt. Express 2, 100–112. doi:https://doi.org/10.1364/BOE.2.000100.

Zaia, J., Annan, R.S., Biemann, K., 1992. The correct molecular weight of myoglobin, a common calibrant for mass spectrometry. Rapid Commun. Mass Spectrom. 6, 32–36. doi:https://doi.org/10.1002/rcm.1290060108.